Phase Noise Analysis of Colpitts and Hartley CMOS Oscillators

Marius Voicu[1,2], Domenico Pepe[1] and Domenico Zito[1,2]

[1]Tyndall National Institute, Lee Maltings, Dyke Parade, Cork

[1,2]Dept. of Electrical and Electronic Engineering, University College Cork

Email:domenico.zito@tyndall.ie

Abstract – This paper reports comparative analyses of the phase noise predictions through Cadence simulations for two LC oscillator topologies: Colpitts and Hartley oscillators. The oscillators have been designed and phase noise performance have been derived by means of both direct Cadence-SpectreRF simulations and the Impulse Sensitivity Function (ISF). All the simulation steps for deriving the ISF have been discussed in detail. The ISF has been evaluated for a wide range of amplitudes of the injected current pulse and compared with simulation results obtained directly by Cadence-SpectreRF simulations. The comparative analyses carried out for a set of different injected pulse amplitudes show that the ISF provides accurate predictions across the entire amplitude range and that the phase noise performance of Colpitts are superior to Hartley oscillator.

Keywords – Oscillators, Phase Noise, Colpitts, Hartley, CMOS, Impulse Sensitivity Function

I INTRODUCTION

Oscillators are extensively used in both transmit and receive paths of RF transceivers. They are a key building block in the Phase-Locked Loop (PLL), and their performances have a strong impact on the performances of the whole communication system [1,2]. Typical performance parameters of an oscillator are its frequency of operation, output swing and phase noise (PN) [3, 4]. Oscillator phase noise (PN) has been studied intensively over the last decades [5-9]. First studies were based on a linear time-invariant (LTI) model of the oscillator. These studies have contributed significantly to a better understanding of phase noise mechanism in oscillators, and have provided important qualitative design insights. However, they are limited in their quantitative prediction of power spectral density levels [10].

A linear time variant (LTV) model for oscillators was introduced in [10]. This model allows a quantitative understanding of oscillator PN. [10] explains the concept of Impulse Sensitivity Function (ISF) of an oscillator. Since the oscillator is assumed to be a linear circuit, it can be completely described in terms of its impulse response. If we apply a current impulse at the input of an LC oscillator, it will produce a step change in the phase of oscillation. Thus, the impulse response can be written as

$$h_{\varphi}(t,\tau)=\frac{\Gamma(\omega_0\tau)}{q_{max}}u(t-\tau) \qquad (1)$$

where q_{max} is the charge injected in the oscillator, $u(t-\tau)$ is the unit step function, and $\Gamma(x)$ is the ISF, which is a dimensionless, frequency and amplitude independent function, periodic in 2π. By the knowledge of the ISF of an oscillator, it is possible to predict its PN [10]. The ISF also allows us to have an insight on the contribution of each noise source of the oscillator circuit to the total PN. This aspect is helpful to the designers to understand how to minimize the PN of an oscillator. [11] presents a detailed procedure to compute the ISF and predict the PN of a source-coupled CMOS multi-vibrator. All the results are achieved for a single amplitude value of the injected impulse oscillators.

Despite new phase and frequency domain methods have been recently proposed to derive the ISF directly from steady state simulations [12], the evaluation of the ISF in the time domain involves a significant amount of simulations, resulting very time consuming. Therefore, a comparative study of

PN predictions based on ISF, for different oscillator topologies, can contribute to get a better understanding about the design of low PN oscillators. Moreover, it could be convenient to know the accuracy of results and how they may be sensitive to the amplitude of the injected impulse.

In this regard, a PN comparative analysis between single-ended Colpitts, differential Colpitts, and cross-coupled differential pair (CCDP) oscillators has been carried out in [13]. That work showed that phase noise performance of CCDP oscillators are superior to those obtained for Colpitts.

In this framework, this paper extends the comparison to two of the most widespread oscillator topologies: Colpitts and Hartley. A comparative study of PN predictions based on ISF calculations and circuit simulations by SpectreRF Periodic Steady State (PSS)-Pnoise simulations for Colpitts and Hartley oscillators has been carried out. All the steps needed for the ISF calculation are clearly explained. Moreover, an insight regarding the contribution to the total phase noise of each noise source of the studied oscillators is provided. Considerations on the proper choice of pulse amplitude and duration for the evaluation of ISF are also provided.

This paper is organized as follows. Section II introduces the two circuit topologies addressed by this paper, highlights their noise sources and shows the simulation steps to derive their ISF and PN prediction. Simulation results and discussions are presented in Section III. Finally, conclusions are drawn in Section IV.

II ISF CALCULATION AND PN PREDICTION IN COLPITTS AND HARTLEY OSCILLATOR

Colpitts and Hartley oscillators have been designed in 0.35 µm CMOS technology by Austriamicrosystems. The two oscillators have been designed to oscillate at the same oscillation frequency (7 GHz) and with the same power consumption (12 mW from a 3-V power supply) for a fair comparison. A quality factor (Q) of 10 has been considered for their inductors.

The Colpitts oscillator (single-ended) is shown in Fig. 1a. Channel length and width of transistors M1 and M2 are 0.35 and 72 µm, respectively. Inductance L is equal to 3.7 nH (Q=10) and capacitors C_1 and C_2 are equal to 100 fF.

The Hartley oscillator (single-ended) is shown in Fig. 1b. The channel length and width of the transistors M1 and M2 are 0.35 and 72 µm, respectively. Inductance L_1 and L_2 are equal to 1 nH (Q=10) and capacitor C is equal to 100 fF.

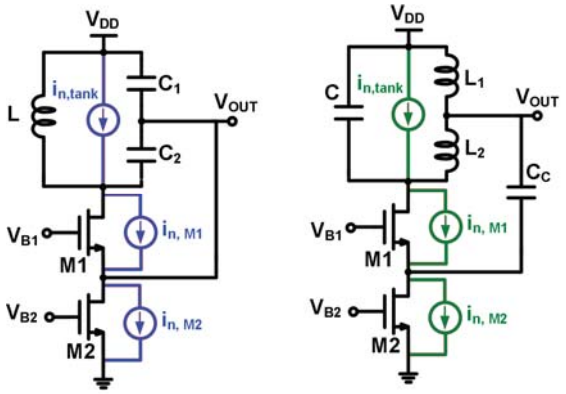

a) b)

Fig. 1. Schematics of the two LC oscillators: a) Colpitts; b) Hartley. Noise sources are highlighted in blue for the Colpitts and green for the Hartley.

Noise sources in the oscillators of Fig. 1 are highlighted in blue for the Colpitts and green for the Hartley. The current source i_n_tank represents the thermal noise associated to the parasitic resistance of the inductors of the tank. Its power spectral density (PSD) is equal to

$$\overline{i_n^2} / \Delta f = 4kT / R_P \qquad (2)$$

where K is the Boltzmann's constant, T is the absolute temperature and R_P is the parallel parasitic resistance of the inductor of the tank.

The current source i_n_Mi (i=1,2) represents the channel white noise current of the transistors. The power spectral density of the channel noise current is given by

$$\overline{i_n^2} / \Delta f = 4kT\gamma\mu C_{ox} \frac{W}{L}(V_{GS} - V_{TH}) \qquad (3)$$

where γ is a bias-dependent noise excess factor (typically 2/3 for long-channel devices and larger for short-channel devices), µ is the electron mobility, C_{OX} is the gate-oxide capacitance per unit area, W is the width of the device, L is the length of the device, V_{GS} is the gate-source voltage, and V_{TH} is the threshold voltage of the device.

The ISF of the oscillators has been calculated, as described in [11]. Details of the steps performed are reported hereinafter.

1) Transient simulations are performed in conservative mode with a maximum time step equal to 10 fs (i.e. much lower than the minimum time shift of the oscillation caused by an impulsive perturbation of the circuit, see hereinafter). After that the oscillation has reached the steady state (i.e. stabilized), a current impulse is applied in parallel to

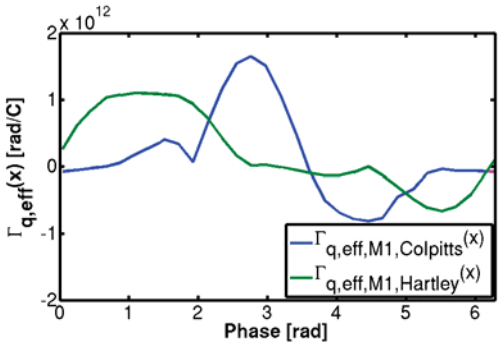

Fig. 2. Simulated $\Gamma_{q,eff}(x)$ curves related to M1 for Colpitts and Hartley oscillators.

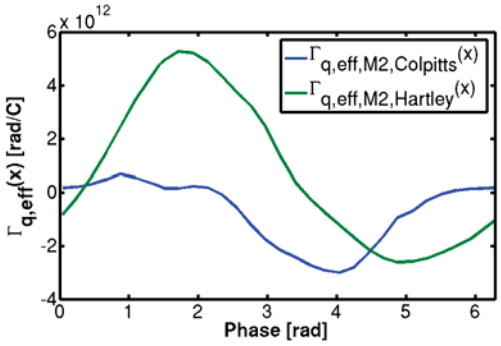

Fig. 3. Simulated $\Gamma_{q,eff}(x)$ curves related to M2 for Colpitts and Hartley oscillators.

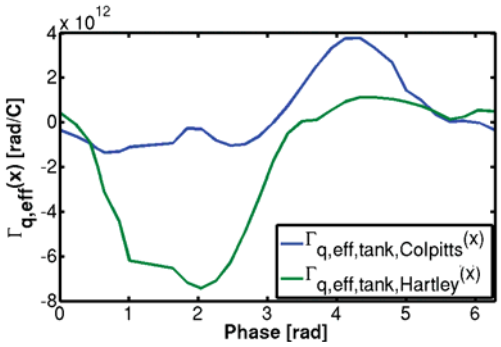

Fig. 4 Simulated $\Gamma_{q,eff}(x)$ curves related to the tank for Colpitts and Hartley oscillators.

a noise source of the oscillator at a certain instant. This is repeated for all the three noise sources, for 30 equally spaced time instants in one oscillation period.

2) After that the oscillation has reached the steady state, the time shift of the zero-crossing between the perturbed oscillation and the unperturbed oscillation is calculated.

3) The time shifts are converted into phase shifts through the relationship $\Gamma(x) = 2\pi(\Delta ti(t)/T)$. This is the ISF.

4) In order to make the result independent from the impulse amplitude (assuming that the impulse is small enough to still have a linear behaviour of the system), the ISF is divided by the charge injected by the current impulses (q_{max} in (1)). The normalized ISF obtained is called $\Gamma_q(x)$.

5) The cyclostationary nature of the noise source is taken into account by evaluating the current flowing into the nodes where the impulses were injected, over an oscillation period. These currents are then normalized by dividing them by their maximum value in the period. The obtained quantity, dimensionless and 2-π periodic, is called $\alpha(x)$.

6) The effective ISF is calculated as $\Gamma_{q,eff}(x)=\Gamma_q(x)\times\alpha(x)$.

7) The root mean square (rms) and dc components of the $\Gamma_{q,eff}(x)$ are calculated for each device. These parameters (Γ_{rms} and Γ_{dc}, respectively) are used to calculate the white noise and flicker noise components of the phase noise.

8) The final step is to compute the total phase noise of the oscillator by adding the contributions of all the noise sources acting in the circuit. The phase noise in the $1/f^2$ region is expressed by [7, 8]

$$L(\Delta\omega) = 10 \cdot log\left(\sum_{n=1}^{3} \frac{\left(\frac{\overline{i_n^2}}{\Delta f}\right)_n \cdot \left(\Gamma_{rms}^2\right)_n}{2 \cdot \Delta\omega^2} \right) \qquad (4)$$

whereas in the $1/f^3$ region it is

$$L(\Delta\omega) = 10 \cdot log\left(\sum_{n=1}^{2} \frac{\left(\frac{\overline{i_n^2}}{\Delta f}\right)_n \cdot \left(\Gamma_{DC}^2\right)_n}{8 \cdot \Delta\omega^2} \cdot \frac{\omega_{1/f}}{\Delta\omega} \right) \qquad (5)$$

where $\omega_{1/f}$ is the flicker noise corner frequency of the MOSFET.

III Simulation Results

The procedure shown in Section 2 has been carried out for the following discrete set of amplitudes of the injected current pulse: 1μA, 10 μA, 100 μA, 1mA and 10mA. The impulse width has been chosen equal to 1 ps, with 0.5 ps rise time and fall time.

The simulated $\Gamma_{q,eff(x)}$ curves for the Colpitts and Hartley oscillators of Fig. 1, related to the noise

Table I. Phase Noise: Summary and Comparison

Oscillator Topology	PHASE NOISE @ 1 MHz [dBc/Hz]					
	SpectreRF simulations	ISF				
		Pulse amplitude 1 µA	Pulse amplitude 10 µA	Pulse amplitude 100 µA	Pulse amplitude 1 mA	Pulse amplitude 10 mA
Colpitts	-107.3	-108.2111	-109.8454	-109.9792	-109.9756	-109.6322
Hartley	-103.8	-104.0934	-104.5234	-104.5697	-104.5665	-104.6389

sources of M1, M2 and the tank, for injected pulse amplitude of 10µA, are shown in Figs. 2-4, respectively.

By using Equations (4) and (5), the phase noise at 1-MHz frequency offset from the carrier is calculated. Since a 1-MHz offset lies in the 1/f2 region of the PN, the term of Equation (4) is largely dominant with respect to that of Equation (5), and thus the latter term can be neglected.

The obtained PN predictions by means of the ISF, and PN obtained by SpectreRF simulations, are reported in Table I.

Table I shows that the results predicted by the ISF calculated as described above are very close to the direct results obtained by means of SpectreRF simulations, for all the current impulse amplitudes of the discrete set chosen, even for the relatively large current amplitudes comparable to the current flowing at the nodes at which is applied. Moreover, Table 1 shows how the Colpitts oscillator exhibits better PN performance with respect to the Hartley oscillators.

IV CONCLUSIONS

The impulse sensitivity function has been used to predict phase noise in two LC oscillator topologies: Colpitts and Hartley. The ISF method has been applied for a wide discrete set of pulse current amplitudes. The predicted phase noise has been compared to the results obtained directly by Periodic Steady State-Pnoise simulations performed by means of SpectreRF. Predicted results are very close to those obtained through direct simulations for all the current pulse amplitudes. Moreover, the comparative analyses show the superior performance in terms of phase noise of the Colpitts oscillator with respect to Hartley oscillator.

ACKNOWLEDGMENTS

The authors are grateful to Science Foundation Ireland (SFI), for their financial support.

REFERENCES

[1] [1] D. Pepe, and D. Zito, “60-GHz Transceivers in Nano-scale CMOS Technology for WirelessHD Standard Applications”, IET Irish Signal and Systems Conference 2012, Maynooth, 28–29 June.

[2] H. Rashtian, and S. Mirabbasi, “Using body biasing to control phase-noise of CMOS LC oscillators”, IET Electronics Letters, vol. 48, no. 3, Feb. 2012.

[3] D. Zito, D. Pepe, “LC-Active VCO for CMOS RF Transceivers”, International Journal of Circuit Theory and Applications, ed. Wiley Interscience, vol. 38, no. 1, pp. 69–84, Feb. 2010.

[4] D. Zito, A. Fonte, D. Pepe, “13-GHz CMOS LC-active Inductor VCO”, IEEE Microwave and Wireless Components Letters, vol. 22, no. 3, pp. 138-140, Mar. 2012.

[5] D.B. Leeson, “A simple model of feedback oscillator noises spectrum”, Proc. IEEE, vol. 54, pp. 329-330, Feb. 1966.

[6] J. Rutman, “Characterization of phase and frequency instabilities in precision frequency sources: Fifteen years of progress”, Proc. IEEE, vol. 66, pp. 1048-1174, Sept. 1978.

[7] A.A. Abidi, R.G. Meyer, “Noise in relaxation oscillators”, IEEE J. of Solid-State Circuits, vol. SC-18, pp. 794-802, Dec. 1983.

[8] B. Razavi, “A study of phase noise in CMOS oscillators”, IEEE J. of Solid-State Circuits, vol. 31, pp. 331-343, Mar. 1996.

[9] A. Buonomo, “Nonlinear Analysis of Voltage-Controlled Oscillators: A Systematic Approach”, IEEE Trans. On Circuits and Systems I, vol. 55, no. 6, July 2008, pp. 1659-1670.

[10] T.H. Lee, A. Hajimiri, “Oscillator phase noise: A tutorial”, IEEE J. of Solid-State Circuits, vol. 35, no. 3, pp. 326-336, Mar. 2000.

[11] M. Paavola, M. Laiho, M. Saukoski, M. Kamarainen, K.A.I. Halonen, "Impulse sensitivity function-based phase noise study for low-power sourced-coupled CMOS multivibrators", Analog Integrated Circuits and Signal Processing, vol. 62, no. 1, pp. 29-41, Jan. 2010.

[12] P. Maffezzoni, "Analysis of Oscillator Injection Locking Through Phase-Domain Impulse-Response", IEEE Transactions on Circuits and Systems I: Regular Papers, vol. 55, no. 5, May 2008, pp. 1297-1305.

[13] X. Wang, P. Andreani, "A phase noise analysis of CMOS colpitts oscillators", Proc. of the Norchip Conference, pp. 151-154, 2004.